Lawrence Berkeley National Laboratory
Recent Work

Title
SURFACE STUDIES BY NONLINEAR OPTICS

Permalink
https://escholarship.org/uc/item/28n8k0dm

Author
Shen, Y.R.

Publication Date
1987-08-01

eScholarship.org   Powered by the California Digital Library
                                                      University of California

Lawrence Berkeley Laboratory

UNIVERSITY OF CALIFORNIA

Materials & Chemical Sciences Division

Surface Studies by Nonlinear Optics

Y.R. Shen

August 1987

TWO-WEEK LOAN COPY

DISCLAIMER

Surface Studies by Nonlinear Optics

Y.R. Shen[*]

Max-Planck-Institut für Quantenoptik

D-8046 Garching, FRG

Abstract

A number of randomly selected examples are presented to show the
versatility of surface optical second harmonic generation
employed as a surface probe. Extension to sum-frequency genera-
tion further allows molecular selectivity in the detection via
surface vibrational spectroscopy.

Surface science is an immense interdisciplinary field of both fundamental and practical importance. The progress of the field, unfortunately, has been impeded by the lack of enough surface analytical tools. With the advent of lasers, one would naturally ask whether lasers can be used as effective probes to study surfaces. In the past several years, we have been working on the development of second-order nonlinear optical processes for surface probing. The results so far have been extremely rewarding.

The basic idea underlying our new surface probing method is quite simple. It is well known that a second-order nonlinear optical process is forbidden under the electric-dipole approximation in media with inversion symmetry, but at a surface or interface, the inversion symmetry is necessarily broken, and therefore, the process is intrinsically surface-specific.[1] However, to be an effective surface probe, it must still satisfy two more requirements. First, it must have enough sensitivity to detect a submonolayer of surface atoms or molecules. Second, it must have enough advantages over the conventional surface probes such as low-energy electron diffraction (LEED), Auger, mass, and electron loss spectroscopy.

That our technique indeed has the submonolayer sensitivity can be seen from an estimate of the second harmonic (SH) signal generated from a monolayer of molecules using the following approximate equation derived from the standard theory[1]:

$$S = [32\pi^3\omega \sec^2\theta/ c^3\epsilon(\omega)\epsilon^{1/2}(2\omega)] \; |\chi_s^{(2)}|^2 \; I^2(\omega) A T \quad \text{photons/pulse}$$

for an input laser pulse with intensity $I(\omega)$, cross-section A, and pulse duration T. Here, ϵ is the dielectric constant, θ is the SH reflection angle, $\chi_s^{(2)} \cong N_s < \alpha^{(2)} >$ is the effective surface nonlinear susceptibility, N_s is the surface density of molecules, and $<\alpha^{(2)}>$ is the molecular nonlinear polarizability averaged over the molecular orientations. Taking $N_s \sim 10^{15}$ /cm^3, $<\alpha^{(2)}> \sim 10^{-30}$ esu for typical molecules, $I(\omega) \sim 10$ MW/cm^2 at 1.06 m, A ~ 0.2 cm^2, T ~ 10 nsec, $\theta \sim 45^o$, and $\epsilon(\omega) \sim \epsilon(2\omega) \sim 1$, we find S $\sim 10^4$ photons/pulse. Such a signal strength is of course fairly easy to detect using a photomultiplier.

Our technique does have a number of advantages over the conven-

tional surface probes. Most of these advantages are intrinsic to the optical methods. First, the experimental setup is simple, at least for second harmonic generation (SHG). Then, by keeping the laser power sufficiently low, the technique is nondetrimental. Because the process employed is coherent and highly directional, the technique can be used for in-situ remote sensing measurements. With lasers as the light sources, it has very high spatial ($\sim 1~\mu$m), time (< 1 psec), and spectral (< 1 cm^{-1}) resolution. Being an optical method, it can be applied to any interface accessible to light. We have experimentally demonstrated the wide applicability and powerfulness of the technique in a large variety of cases involving various types of interfaces. In the following, we briefly discuss a few randomly selected examples to illustrate the strength of this novel surface probe.

The definitive experiment necessary to convince experts in surface science about the new technique is the detection of molecular monolayers on metals and semiconductors in ultrahigh vacuum (UHV). We have used SHG to study CO adsorption on Rh(III).[2] This is a technologically important problem since CO and H$_2$ on transition metals often lead to the catalytical formation of hydrocarbons. Figure 1 shows that as the surface coverage, θ , of CO increases, the SH signal drops monotonically. In the experiment, the surface coverage was calibrated by LEED. The data exhibit a kink at θ = 1/3. It is a manifestation of the fact that CO can appear only on Rh(III) at the top sites for θ < 1/3 and can appear at both the top sites and the bridge sites for 1/3 < θ < 3/4. The data can actually be fit by the following simple expression for $\chi_s^{(2)}$ based on the above picture.

$$\chi_s^{(2)} = A~(1 - \theta/\theta_s) + B~\theta/\theta_s \qquad \text{for } \theta \leqslant 1/3$$
$$= A~(1 - \theta/\theta_s) + (1/3)B/\theta_s + C~(\theta - 1/3)/\theta_s \quad \text{for } 1/3 < \theta < 3/4$$

with the saturation coverage θ_s = 3/4. Here, A, B and C are constant coefficients; the A term refers to the contribution from the base metal part of the surface. This experiment shows that surface SHG indeed has the sensitivity of detecting a submonolayer of diatomic molecules, and furthermore, it is even sensitive to the different adsorption sites. The decrease of the SH signal upon CO adsorption results from electron localization by

the chemiadsorption of CO on Rh(III).

We have also succeeded in using SHG to monitor the oxidation of Si surfaces and the subsequent desorption of oxygen from the surfaces by heating.[3] The results are shown in Fig. 2. The originally clean Si(III) sample was placed in an UHV chamber. Leaking of oxygen into the chamber caused a decay in the SH signal, presented in Fig. 2(a). This was due to quenching of the highly nonlinear dangling bonds on the surface by oxygen adsorption. Upon heating of the sample at 900° C, the signal was recovered as oxygen was desorbed, as depicted in Fig. 2(b). In both adsorption and desorption, the experimental results can be fit by the simple Langemuir kinetic model which predicts that the oxygen surface coverage takes the form

$$\theta = \theta_s \, [1 - \exp(-kt)] \qquad \text{for adsorption}$$
$$= \theta_s \, \exp(-k't) \qquad \text{for desorption}$$

together with a surface nonlinear susceptibility given by

$$\chi_s^{(2)} = A \, (1 - \theta/\theta_s) + B \, \theta/\theta_s.$$

This example shows that SHG can be used to monitor the dynamics of molecular adsorption and desorption on a surface.

Unlike many other surface probes, our nonlinear optical technique is not restricted to surfaces in vacuum. As an example to illustrate the applicability to liquid/solid interfaces, we consider the case of adsorption of p-nitrobenzoic acid (PNBA) at the ethanol/silica interface.[4] The SH signal was found to be mainly coming from the adsorbed PNBA. As the PNBA concentration in ethanol increased, the signal increased accordingly, but soon saturated because of saturation of adsorption. This is shown in Fig. 3. From this measured adsorption isotherm, the free energy of adsorption of PNBA on silica from ethanol can be deduced (8 KCal/mole).

As with other optical methods, the polarization dependence of SHG allows us to deduce the molecular orientation on surfaces. The basic idea is simple. The nonlinear susceptibility tensor $\chi_s^{(2)}$

is related to the nonlinear polarizability tensor $\alpha^{(2)}$ of the molecules by a coordinate transformation that depends on the molecular orientation (assuming the microscopic local field is negligible)

$$(\chi_s^{(2)})_{ijk} = N_s < G_{ijk}^{\xi\eta\zeta}(\theta) > \alpha_{\xi\eta\zeta}^{(2)}$$

where $G_{ijk}^{\xi\eta\zeta}(\theta)$ is the geometric factor specified by the coordinate transformation from the molecular coordinates (ξ,η,ζ) to the lab coordinates (i,j,k) with θ describing the molecular orientation (specified by three Euler angles in general) and the angular brackets indicate an average over all the molecules. If $\alpha_{\xi\eta\zeta}^{(2)}$ are known and $(\chi_s^{(2)})_{ijk}$ can be measured, then $<G_{ijk}(\theta)>$ and hence the wighted average orientation of the molecules can be deduced. In simple cases where a single element of $^{(2)}$ dominates, the procedure is straight-forward. Let us take again the adsorption of PNBA on fused silica as an example.[4] In this case, the molecular nonlinear polarizability is dominated by $\alpha_{\xi\eta\zeta}^{(2)}$ with pointing along the long molecular axis which has a random azimuthal distribution. We can then easily show that

$$\chi_{s,zzz}^{(2)} = N_s \alpha_{\zeta\zeta\zeta}^{(2)} < \cos^3\theta >$$
$$\chi_{s,zxx}^{(2)} = \chi_{s,xzx}^{(2)} = 1/2\ N_s \alpha_{\zeta\zeta\zeta}^{(2)} < \sin^2\theta\cos\theta)$$

where θ is now the angle between $\hat{\zeta}$ and the surface normal $\hat{z}$. Thus, by measuring the ratio of $\chi_{s,zzz}^{(2)} / \chi_{s,zxx}^{(2)}$, for example, we can obtain a value for $<\cos^3\theta> / <\sin^2\theta\cos\theta>$, and if the orientational distribution is sufficiently sharp so that it can be approximated by a δ-function, we can then deduce a value for θ. Using this approach, we find $\theta \simeq 38°$ for PNBA at the ethanol/silica interface. Similar measurements for PNBA adsorbed at the air/silica interface yield $\theta \simeq 70°$. This is understandable considering that the dielectric effect of the ethanol solution would tend to orient the PNBA molecules more towards the surface normal.

The measurements of molecular orientations using SHG can also be applied to Langmuir films ------ molecular monolayers adsorbed on water. We have used the technique to study the so-called liquid-expanded (LE) to liquid-compressed (LC) phase transition of such

a two-dimensional system.[5] As seen in Fig. 4 for pentadecanoic acid (PDA) the phase transition at a constant temperature is characterized by a kink in the (surface tension) -- A (surface area) curve, but the nature of this transition is not clearly understood. It has been suggested that the transition may involve a sudden change in the molecular orientation. With our technique, we could now measure the molecular orientation as a function of A (or N_s). The results are shown in Fig. 5. Indeed, the transition is characterized by an orientational change, as evidenced by the kink coinciding with the beginning of the phase transition. For PDA, the molecular nonlinear polarizability is dominated by $\alpha_{\hat{\zeta}\hat{\zeta}\hat{\zeta}}^{(2)}$ with $\hat{\zeta}$ along the CO double bond, and therefore θ here denotes the polar angle of the CO bond. In a closely packed monolayer, we expect the hydrocarbon chain of the molecules to stand up vertically, and correspondingly, the CO bond should approach a tilt angle of 60° with respect to the surface normal. The results in Fig. 5 show that this is actually the case.

Since pulsed lasers are used in our technique and the nonlinear optical response is nearly instantaneous, we can apply the technique to the dynamic studies of surface reactions. As an illustration, we consider polymerization of a monolayer of monomers initiated by UV irradiation.[6] Monolayer polymerization is a problem of fundamental interest, because of its reduced dimensionality. By spreading the monomers on water, one can also study how the polymerization process is affected by a change of the surface density of the monomers. Figure 6 shows how the SH signal responds to the polymerization by UV irradiation of a full monolayer of octadecyl methacrylate spread on water. The signal decays upon polymerization because in the process the more nonlinear C = C double bond is reduced to two less nonlinear single bonds. The experimental results in Fig. 6 can in principle be used to test the various theoretical models of polymerization.

The possibility of detecting adsorbed molecular monolayers on surface with good spatial resolution limited only by optical diffraction suggests that SHG can be employed for monolayer surface microscopy.[7] Figure 7 provides an example[8]; the picture was obtained by a two-dimensional scan of SHG from a monolayer of dye molecules adsorbed on a fused silica substrate. It shows the pre-

sence of an $8-\mu$m hole which was burned on the monolayer by a focussed laser beam. The resolution limit of such a microscope can be in the submicron range.

Surface monolayer spectroscopy is also possible with SHG. Transitions can be detected via resonant enhancement which occurs when either ω or 2ω approaches a resonance. Figure 8 is an example which exhibits the resonant enhancement of SHG from a half monolayer of Rhodamine 6G and Rhodamine 110 when 2ω scans over the $S_0 \rightarrow S_s$ transitions of the molecules.[9] The shift of the resonant peaks due to the slight structural difference between the two molecules is clearly observed.

In surface science, surface spectroscopy on electronic transitions of adsorbates is often not as interesting as the surface vibrational spectroscopy. This is because the latter provides a more selective detection of adsorbed molecules as the vibrational spectrum is generally regarded as the fingerprint of molecules. Unfortunately, vibrational resonances are in the infrared, where the detection of SHG is far less sensitive owing to the lack of photomultipliers. The use of sum-frequency generation (SFG), instead of SHG, however overcomes all the difficulties. A tunable IR laser beam scans over the surface vibrational resonance and mixes with a visible laser beam to generate a sum-frequency signal in the visible, which can then be detected by a photomultiplier. Since this is still a second-order optical process, surface specificity remains.

We have demonstrated successfully the possibility of performing surface vibrational spectroscopy using SFG in both the 10 μm range[10] and the 3 μm range.[11] An example is shown in Fig. 9, where the spectra of the CH_3 stretches of the end group of pentadecanoic acid are presented.[12]. The molecules were spread on water to form a closely packed monolayer. The different spectra in Fig. 9 refer to different polarization combinations. the peaks at 2880 cm^{-1} and 2960 cm^{-1} are identified as the CH_3 (symmetric) and CH_3 (antisymmetric) stretches, respectively. The peak at 2940 cm^{-1} is likely due to Fermi resonance. The signal dependence on the polarization combination allows us to deduce the orientation of the CH_3 group. We found that the CH_3 axis is tilted at

35° from the surface normal. Knowing that for a straight hydrocarbon chain of PDA, the CH_3 axis should be inclined at 35° with respect to the chain, we conclude that for the full monolayer of PDA, the long hydrocarbon chain of PDA is oriented vertically on the water surface. This confirms the picture we have described earlier. The spectral lines of the CH_2 stretches are absent in the spectra of Fig. 9. This is because on the straight hydrocarbon chain, the CH_2 groups are nearly symmetrically located so that their contributions to SFG are almost cancelled by one another. With lower surface densities, the chain could bend, and consequently the CH_2 stretches would show up in the spectrum as we have indeed observed.

In summary, we have shown that SHG is a very versatile surface probe. It can be applied to all types of interfaces accessible by light with high spatial, time, and spectral resolutions. The intrinsic subpicosecond time response of the process is particularly attractive, as it can be useful for in-situ surface dynamics and catalytical reaction studies. The technique is how ever limited in molecular selectivity. This can be remedied by an extension of the technique to IR-visible sum-frequency generation.

Acknowledgement

References

1. See, for example, Y.R. Shen, "The Principles of Nonlinear Optics", (J. Wiley, New York, 1984), Chapter 25.

2. H.W.K. Tom, C.M. Mate, X.D. Zhu, J.E. Crowell, T.F. Heinz, G.A. Somorjai, and Y.R. Shen, Phys.Rev.Lett. 52, 348 (1984)

3. H.W.K. Tom, X.D. Zhu, Y.R. Shen, and G.A. Somorjai, Surf.Sci. 167, 167 (1986).

4. T.F. Heinz, H.W.K. Tom, and Y.R. Shen, Phys.Rev. A28, 1883 (1983).

5. Th. Rasing, Y.R. Shen, M.W. Kim, and S. Grubb, Phys.Rev.Lett. 55, 2903 (1985).

6. G. Berkovic, Th. Rasing, and Y.R. Shen, J.Chem.Phys. 85, 7374 (1986).

7. G.D. Boyd, Y.R. Shen, and T.W. Hänsch, Optics Lett.

8. Constesey of G.D. Boyd

9. T.F. Heinz, C.K. Chen, D. Ricard, and Y.R. Shen, Phys.Rev.Lett. 48, 478 (1982).

10. X.D. Zhu, H. Suhr, and Y.R. Shen, Phys.Rev. B35, 3047 (1987).

11. J.H. Hunt, P. Guyot-Sionnest, and Y.R. Shen, Chem.Phys.Lett. 133, 189 (1987).

12. P. Guyot-Sionnest, J.H. Hunt, and Y.R. Shen (to be published).

Figure Captions

Fig. 1   SH intensity from   Rh(III) versus CO coverage on
         Rh(III). The solid curve is a theoretical fit.

Fig. 2   SH intensity from Si(III) versus (a) oxygen exposure in
         Langmuir units with the sample at room temperature and
         at 800° C respectively, and (b) desorption time as a
         thermally grown oxide layer desorbs from the surface
         when the sample was held at 900° C.   The dashed curves
         are theoretical fits.

Fig. 3   Isotherm for adsorption of PNBA on fused silica out of
         an ethanol solution obtained by SHG measurements.

Fig. 4   Surface pressure versus area per molecule at three dif-
         ferent temperatures for a monolayer ·of pentadecanoic
         acid molecules spread on water.

Fig. 5   Orientation of the C = O bond of the PDA molecules on
         water as a function of the surface density of the mole-
         cules.

Fig. 6   SH intensity versus irradiation time for UV polymeri-
         zation of octadecyl methacrylate. The dotted and dashed
         curves are theoretical fits derived from two different
         models (see Ref. 6).

Fig. 7   A two-dimensional SHG scan of a dye-monolayer-covered
         quartz plate exhibiting an 8-μm hole burned on the
         monolayer by a focused laser spot.

Fig. 8   Resonant SHG in rhodamine 6G and rhodamine 110: (a) The
         resonant process in the two dyes with energy levels
         corresponding to the absorption line center for the
         molecules dissolved in ethanol; (b) the experimental SH
         spectrum in the region of $S_0 \longrightarrow S_2$ transition for sub-
         monolayers of the dye molecules adsorbed on fused
         silica.

Fig. 9   SFG spectra of PDA at full monolayer coverage using various polarization combinations. 1) s-visible, p-IR; 2) p-visible, s-IR; 3) p-visible, p-IR.
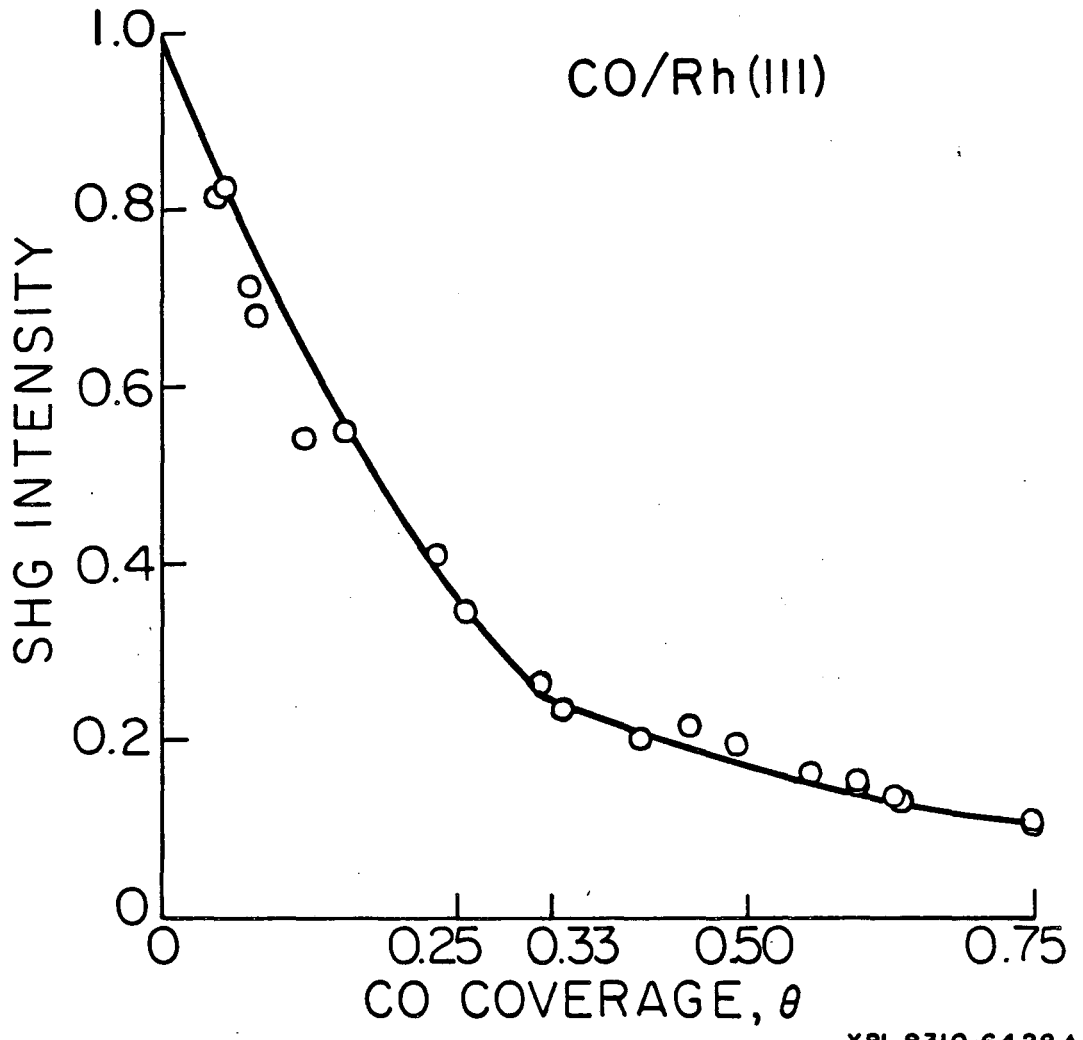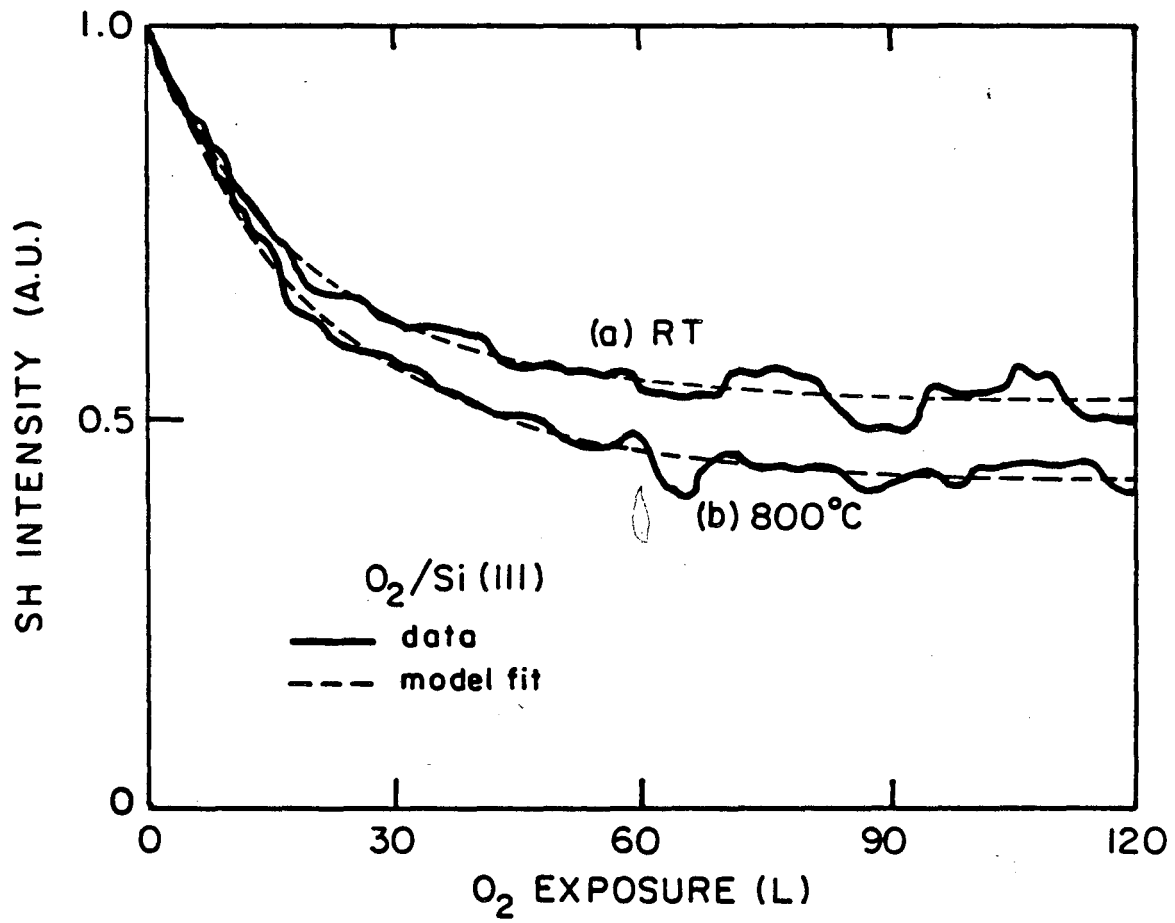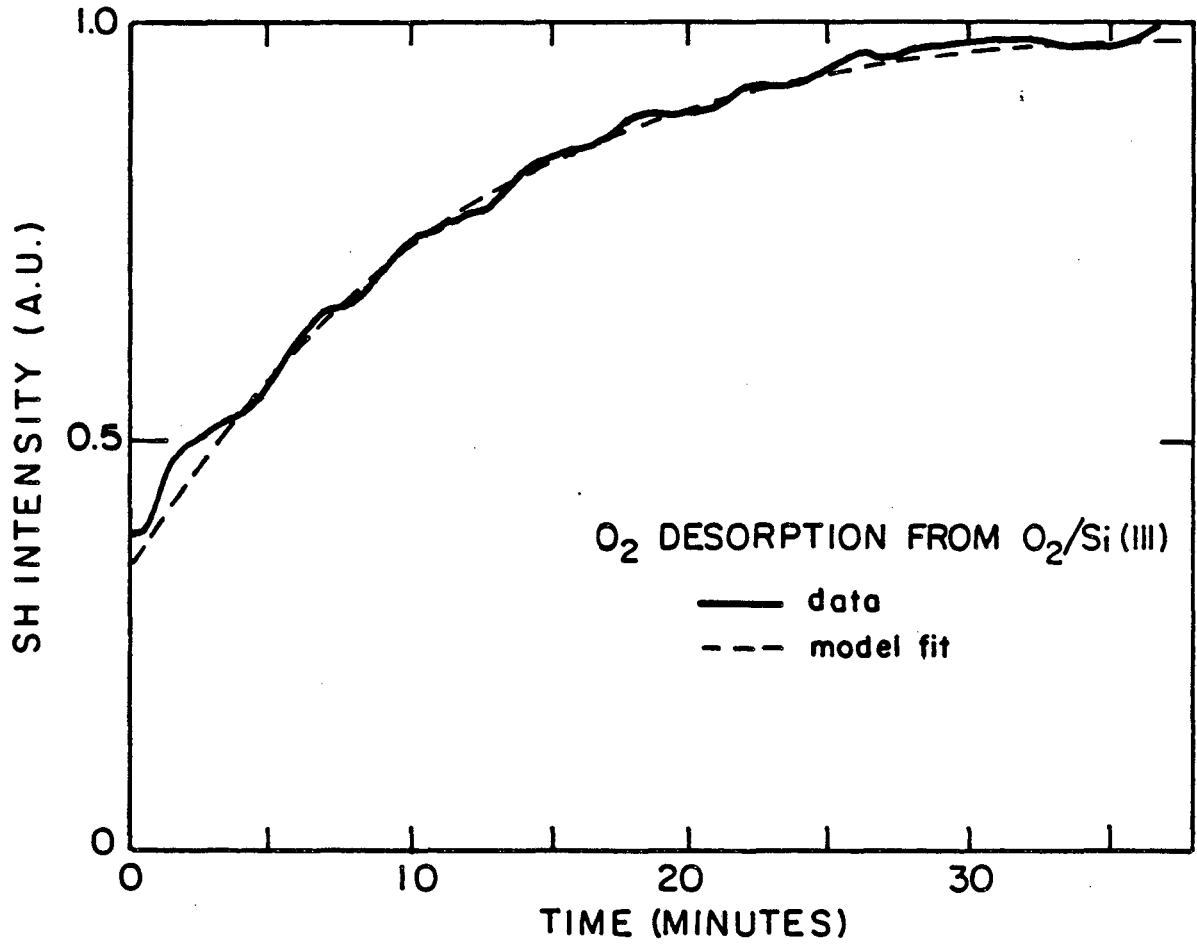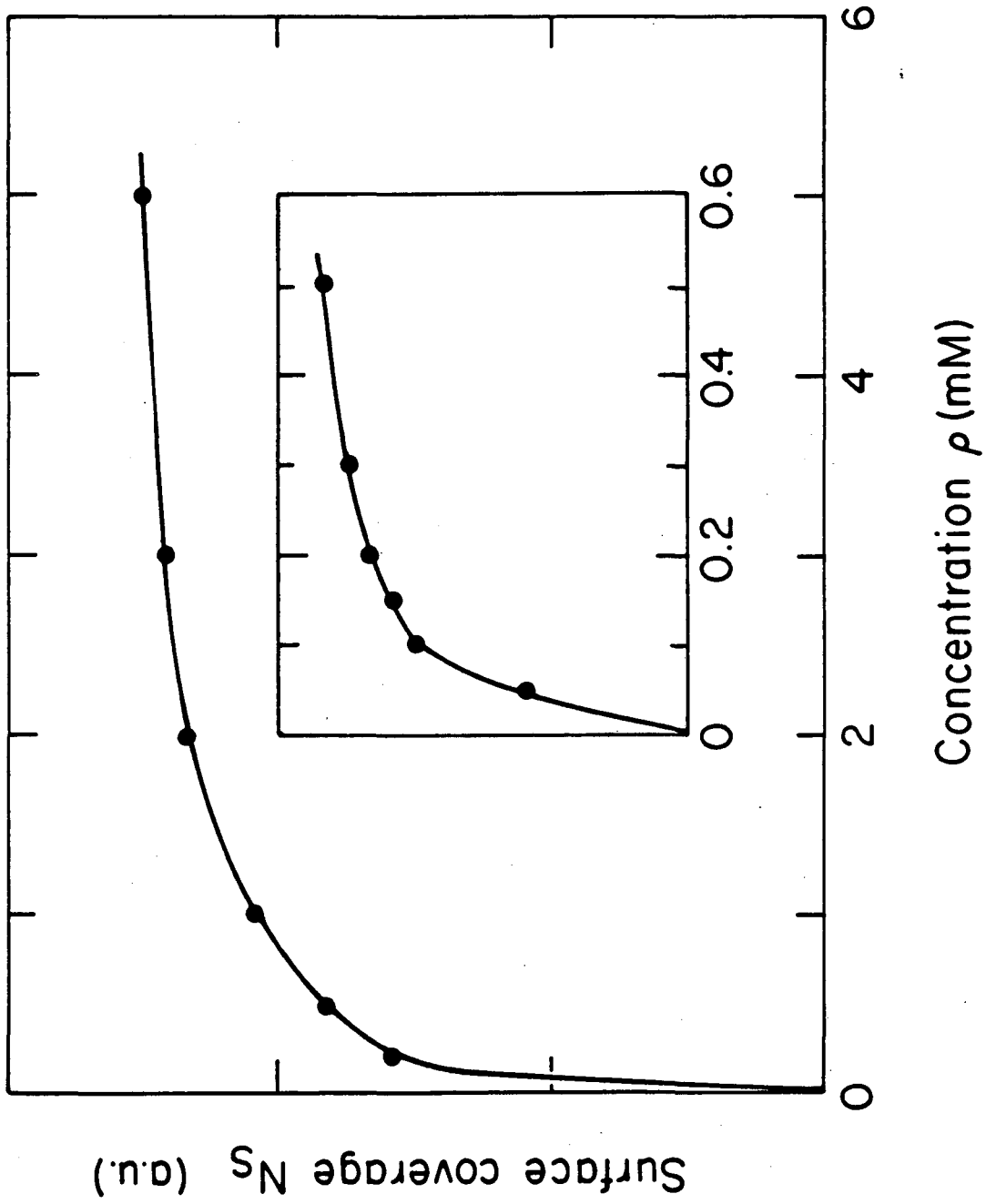
CO/Rh(III)

XBL 8310-6428A

Fig. 1

XBL854-6115

Fig. 2(a)

XBL 854-6116
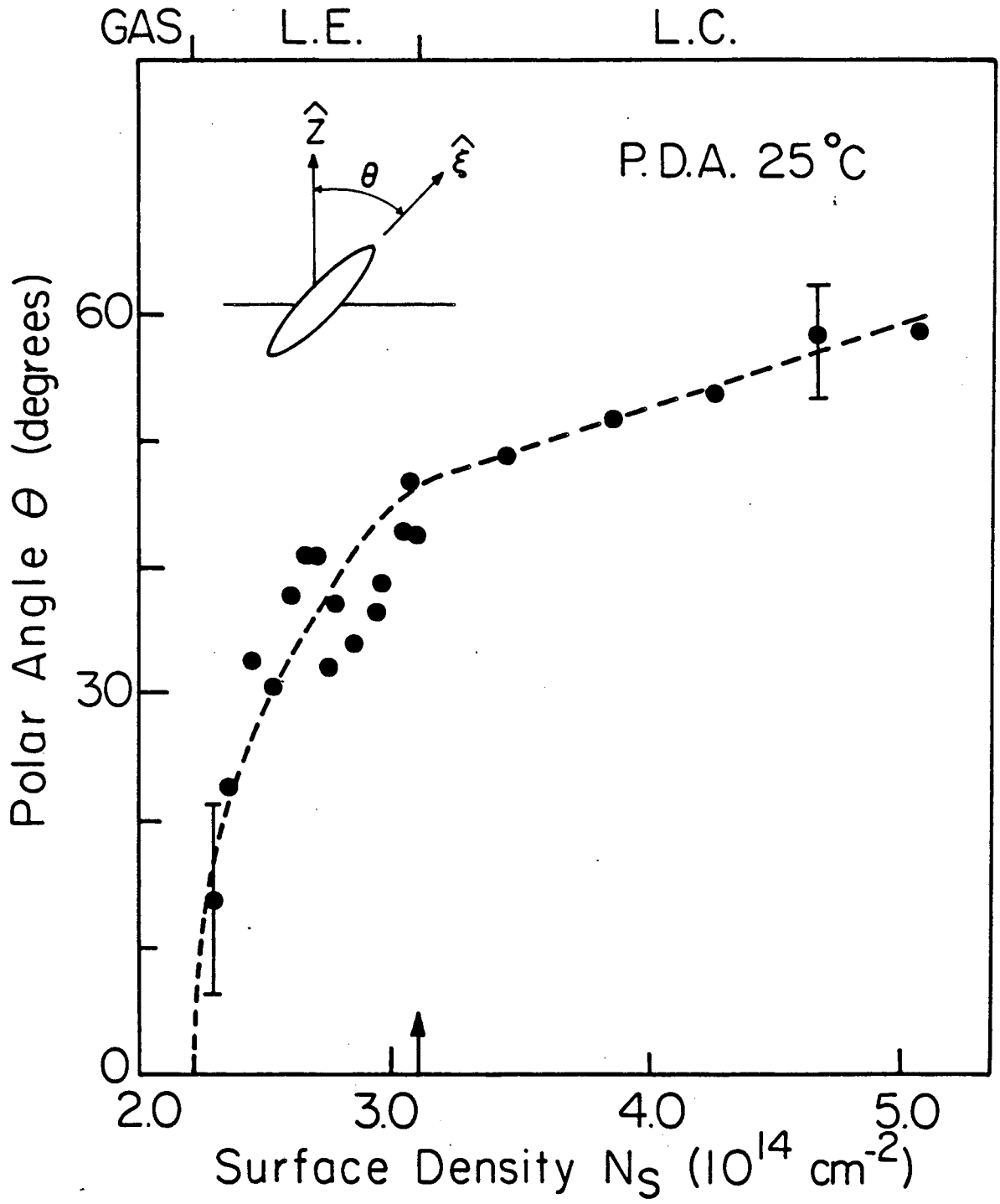
Fig. 2(b)

Concentration ρ (mM)

Surface coverage N_S (a.u.)

XBL 8212-7391

Fig. 3

XBL 856-6356

Fig. 4

Fig. 5

XBL 857-6419

S

Irradiation Time (min)
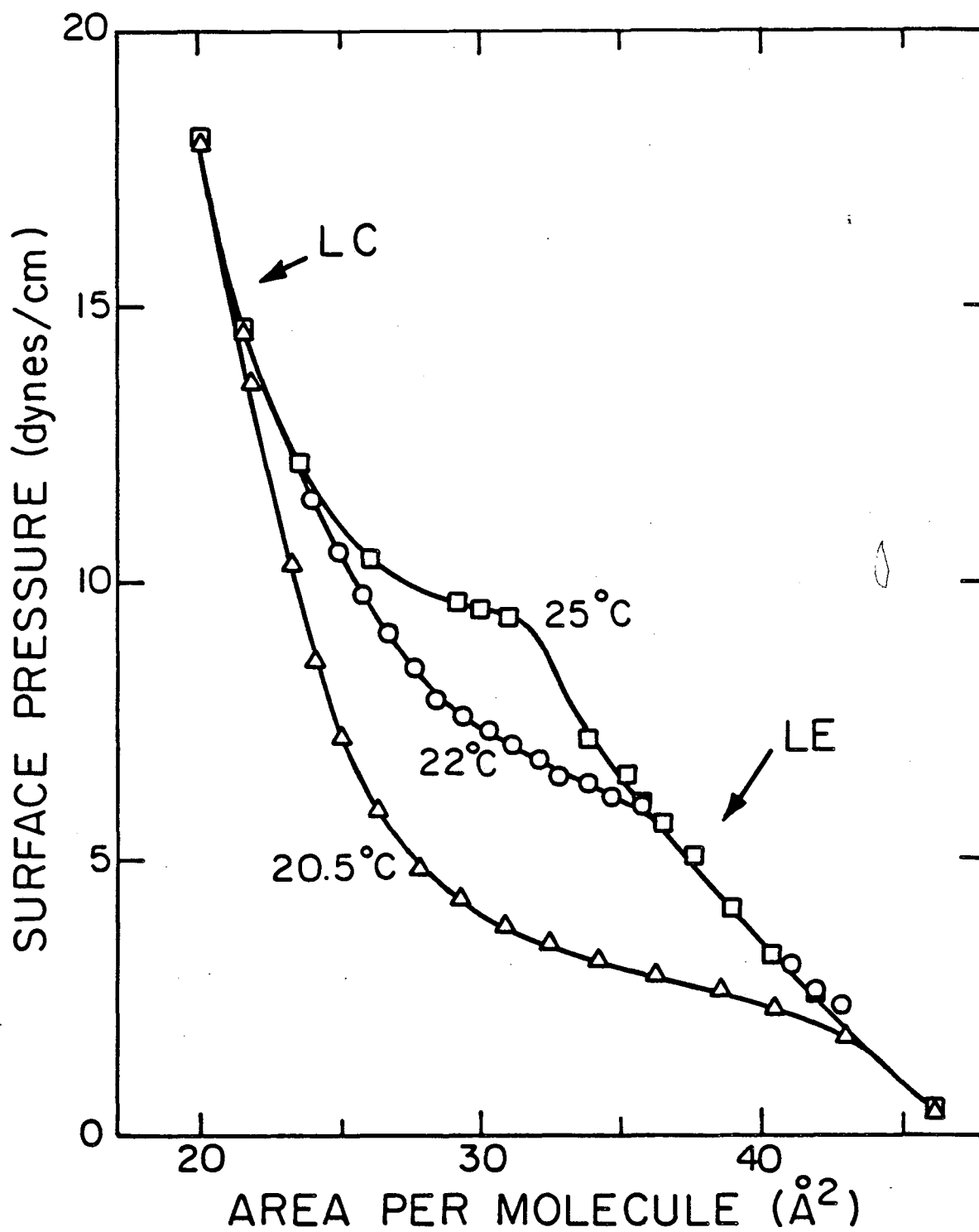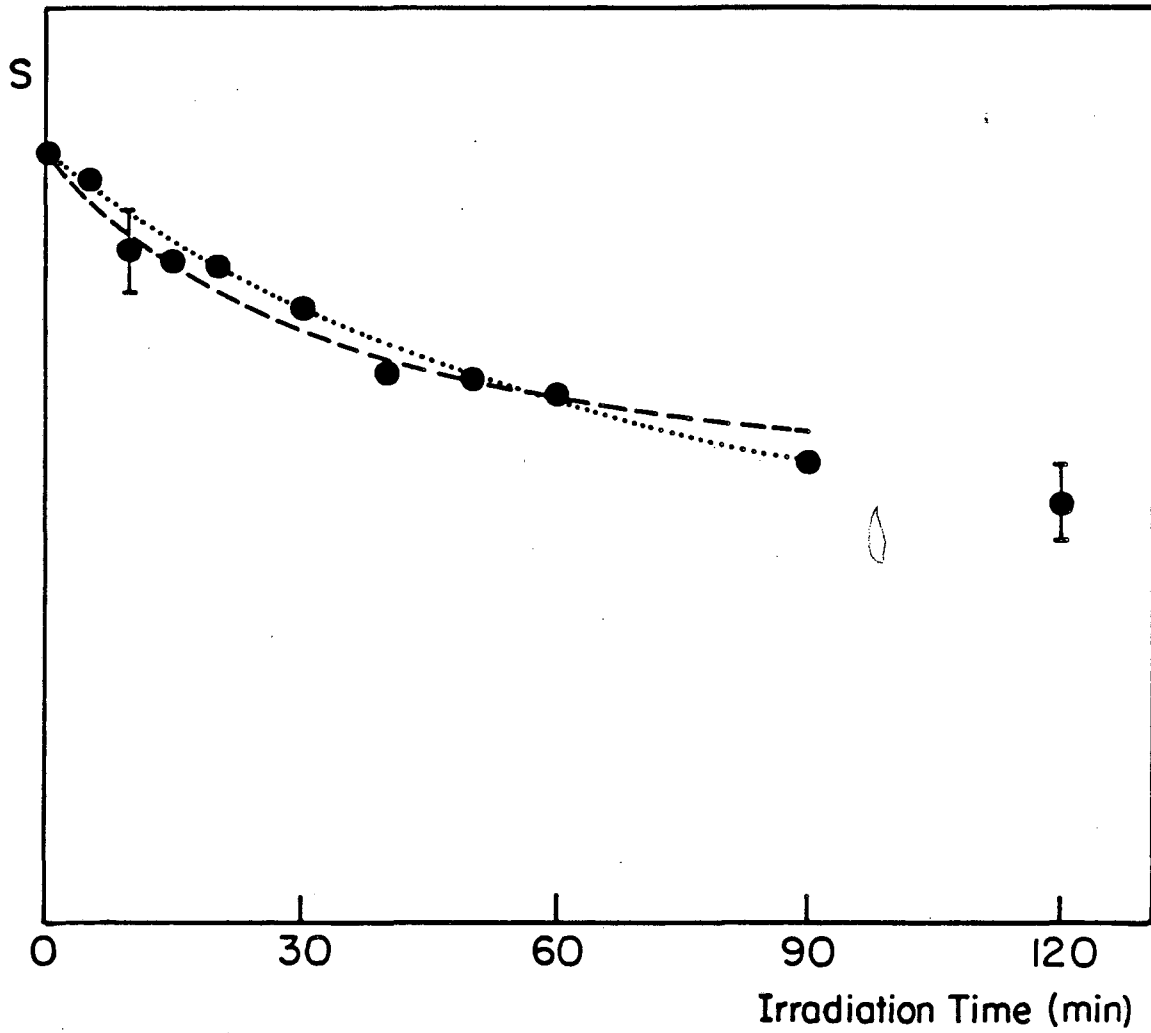
XBL 866-7701

Fig. 6

XBL 8512-6878

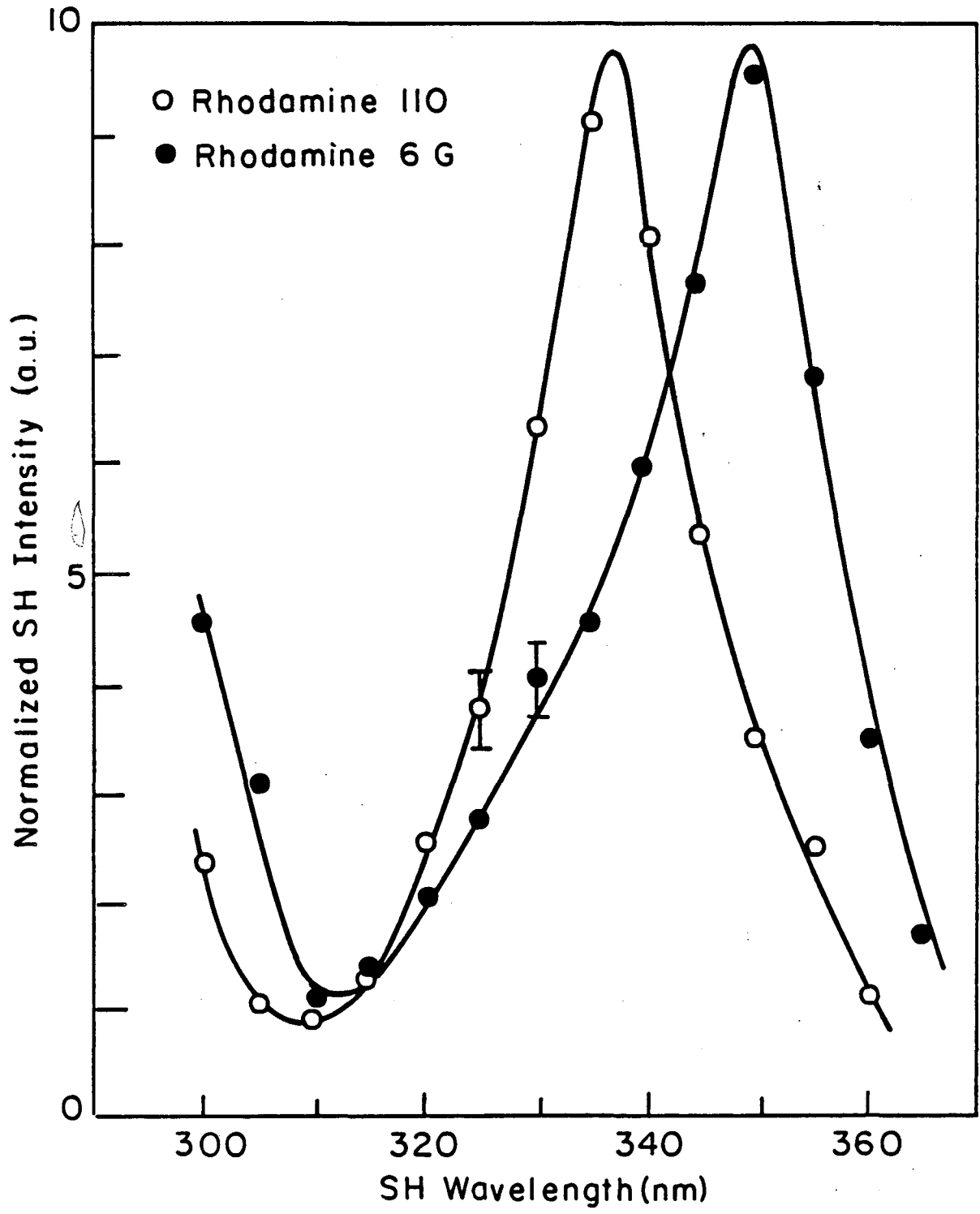Fig. 7

Rhodamine 110   Rhodamine 6G

XBL 8111-12843

Fig. 8(a)

-20-
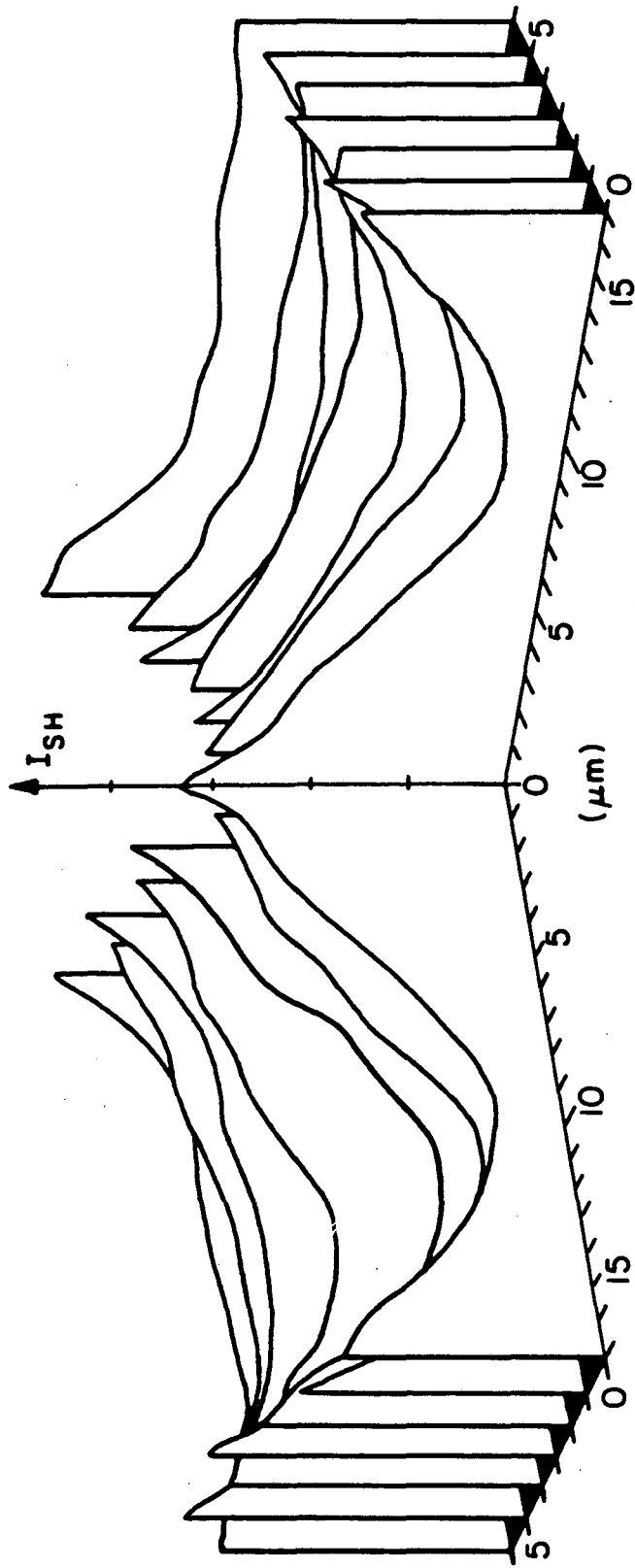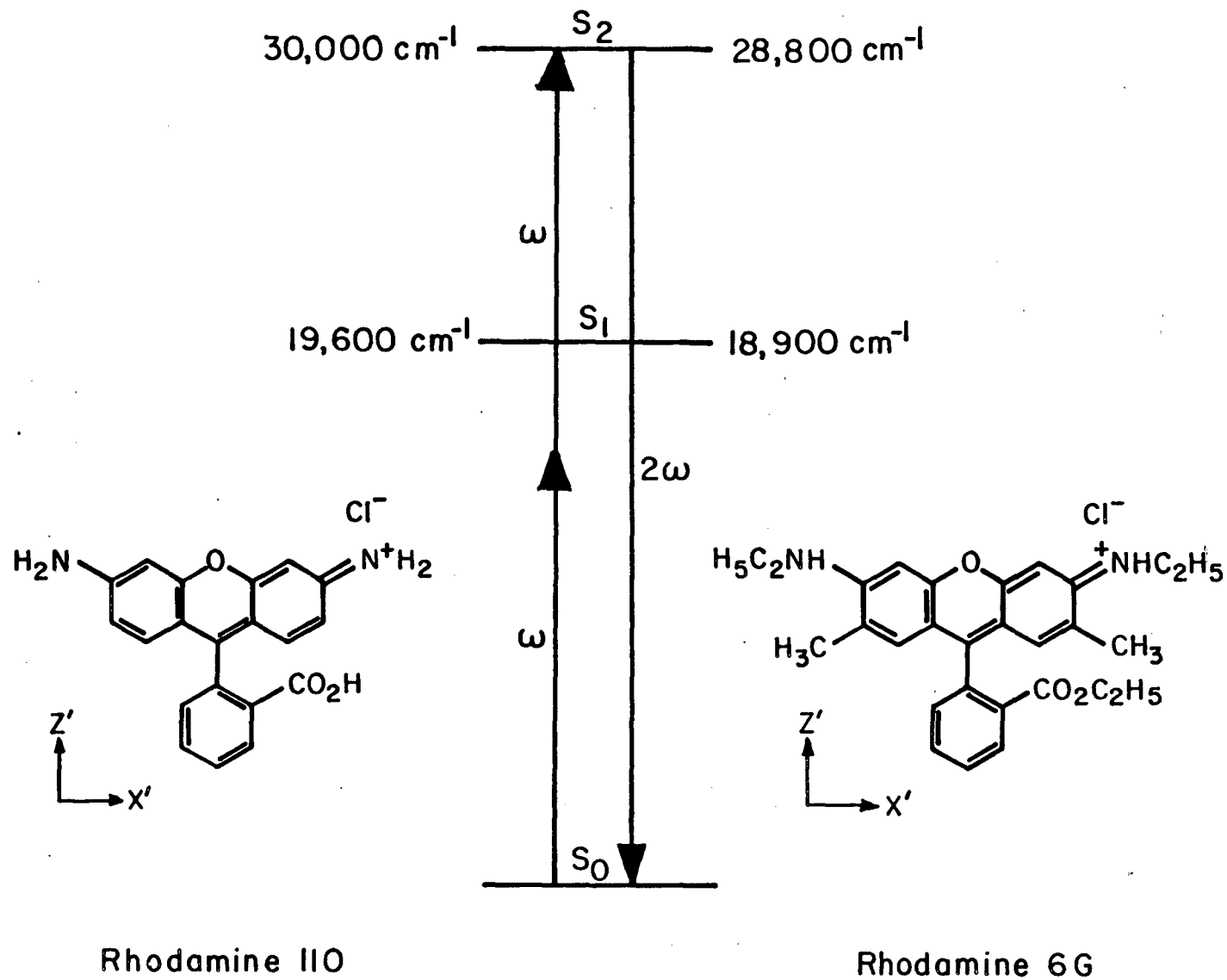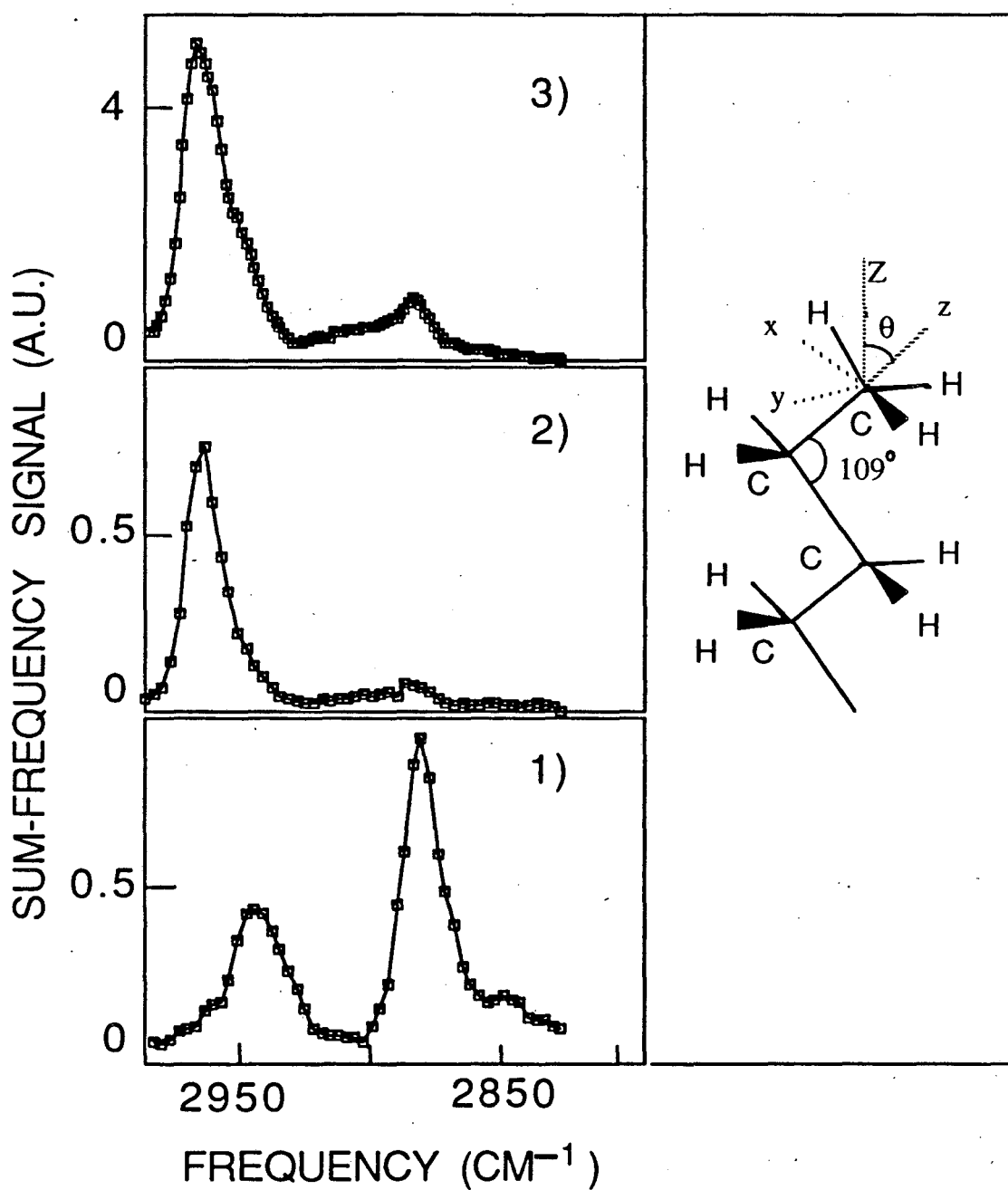
Fig. 8(b)

XBL 8110-6773

XBL 877-3071

Fig. 9

LAWRENCE BERKELEY LABORATORY
TECHNICAL INFORMATION DEPARTMENT
UNIVERSITY OF CALIFORNIA
BERKELEY, CALIFORNIA 94720